Journal of Sound and Vibration (2002) **255**(4), 635–662
doi:10.1006/jsvi.2001.4182, available online at http://www.idealibrary.com on IDEAL®

PARAMETRIC STABILIZATION OF A GYROSCOPIC SYSTEM

R. J. McDonald

Boeing Satellite Systems, Inc, 2260 E. Imperial Highway, El Segundo, CA 90245, U.S.A.

AND

N. Sri Namachchivaya

Department of Aeronautical and Astronautical Engineering, University of Illinois at Urbana-Champaign, 306 Talbot Laboratory, 104 South Wright Street, Urbana, IL 61801-2935, U.S.A.

(*Received* 11 *June* 1999, *and in final form* 19 *November* 2001)

This paper studies the stabilization of a gyroscopic system using parametric stabilization near a combination resonance. The gyroscopic system is near its primary instability, i.e., the bifurcation parameter is such that the system possesses a double zero eigenvalue. The stability of the system is studied for the linear Hamiltonian system, the damped linear system, the forced linear Hamiltonian system, and finally the damped and forced linear system. The addition of the periodic excitation near the critical combination resonance provides the system with an extended stability region when the excitation frequency is slightly above the combination resonance. A non-linear numerical example shows that these results may persist for the non-linear problem. The results of this work, are then discussed in relation to an example gyroscopic problem, a rotating shaft with periodically perturbed rotation rate.

1. INTRODUCTION

Many engineering problems may be classified as *gyroscopic* systems. Gyroscopic forces may arise in an engineering problem through Coriolis forces, Lorentz forces, etc. Hydroelastic and rotating systems, such as pipes conveying fluid and rotating shafts, are examples of engineering problems in which gyroscopic forces occur. Such systems may be parametrically excited by such effects as pulsating fluid flow, periodically varying shaft rotation rate, or pulsating axial thrust. Stability analyses of parametrically excited linear and non-linear gyroscopic systems have been studied by Ariaratnam and Sri Namachchivaya [1, 2]. In these works, the parametric stability was investigated when the unperturbed system was orbitally stable. The addition of parametric periodic perturbations gave rise to subharmonic and combination resonances. The bifurcations associated with these resonances were then investigated.

When the unperturbed gyroscopic system is *not orbitally stable*, the problem becomes more difficult to study. Such cases occur when the unperturbed system possesses resonant eigenvalues along the imaginary axis of the complex plane. The 1 : 1 resonance and the 1 : 2 resonance cases have been studied previously. The so-called "0 : 1 resonance" occurs when the system possesses a pair of eigenvalues near zero in the complex plane. In this case, the frequency of these eigenvalues is very small compared to all other frequencies in the system.

0022-460X/02/$35.00

For simplicity, we will consider the resonance between this double zero eigenvalue and the lowest non-zero frequency in the system. Thus, we shall consider two-degree-of-freedom systems obtained by truncating the set of ordinary differential equations obtained by Galerkin reduction of a continuous physical system. A more sophisticated center manifold analysis would rigorously justify this truncation.

The 0 : 1 resonance problem has been studied extensively in the last few years, both for gyroscopic and non-gyroscopic systems. For non-gyroscopic systems, Nayfeh and co-workers [3, 4] and Feng and Liew [5] have studied the presence of the 0 : 1 resonance in certain structural systems. Sri Namachchivaya and co-workers [6–8] have investigated gyroscopic systems near a 0 : 1 resonance. In reference [6], the authors study both the 0 : 1 resonance and the 1 : 1 resonance for gyroscopic systems without periodic excitations, using nearly symmetric rotating shafts as their primary example. Even without forcing in their system, they found a rich variety of global bifurcations in these systems. McDonald [9] has studied the local and global bifurcations for parametrically excited gyroscopic systems, using rotating shafts and pipes conveying fluid as motivating examples.

In this paper, we examine the dynamics of a damped gyroscopic system with certain symmetries, which is subject to small periodic excitations. The stability characteristics of an undamped, unforced linear gyroscopic system are well known. Namely, an initially stable gyroscopic system can be destabilized and re-stabilized by increasing a bifurcation parameter in the system. This re-stabilization does not occur in real physical problems, however, since damping is always present. In particular, we study a two-degree-of-freedom gyroscopic system close to its primary instability, i.e., the bifurcation parameter is such that the system possesses a pair of pure imaginary eigenvalues and a pair of non-semisimple zero eigenvalues. For such a case, we shall show that if the parametric excitation is near a combination resonance, the stability boundaries of the system may be extended. The usefulness of this expanded stability region can be understood by considering the physical example of the rotating shaft. The expanded stability region due to the parametric excitation would allow the shaft to operate at higher rotation rates than an unexcited shaft, allowing for performance gains in the system.

The extent to which we can predict the extended stabilization region due to parametric periodic perturbations is limited by the perturbative methods used in this paper. To the authors' knowledge, it is the first such result based purely on a linear analysis. In the subsequent analysis, we add the necessary non-linearities and show numerically that such stability may persist even in the presence of non-linearities. In the final section of the paper, we apply this result to a rotating shaft system, and interpret the results in that context.

2. EQUATIONS OF MOTION

A dynamical system is defined as a gyroscopic system if it possesses terms of the form $G_{i,j}\dot{q}_j$, where $G_{i,j} = -G_{j,i}$. Since we are dealing with discretized equations of motion, this property becomes $G = -G^{\mathrm{T}}$. Thus, a general form of the equations of motion for a damped gyroscopic system can be written

$$\ddot{q} + 2G(t)\dot{q} + \dot{G}(t)q + Kq + \nabla U(q, t) + \zeta[\Lambda\dot{q} + F(q, \dot{q})] = 0, \tag{1}$$

where $q \in \mathbb{R}^d$ is a generalized co-ordinate. The symmetric matrix K represents linear stiffness terms in the equations of motion arising from the potential energy. The function $\nabla U(q, t)$ contains non-linear terms arising from the potential energy, as well as parametric excitation terms. Matrix Λ and the function F represent linear and non-linear terms arising

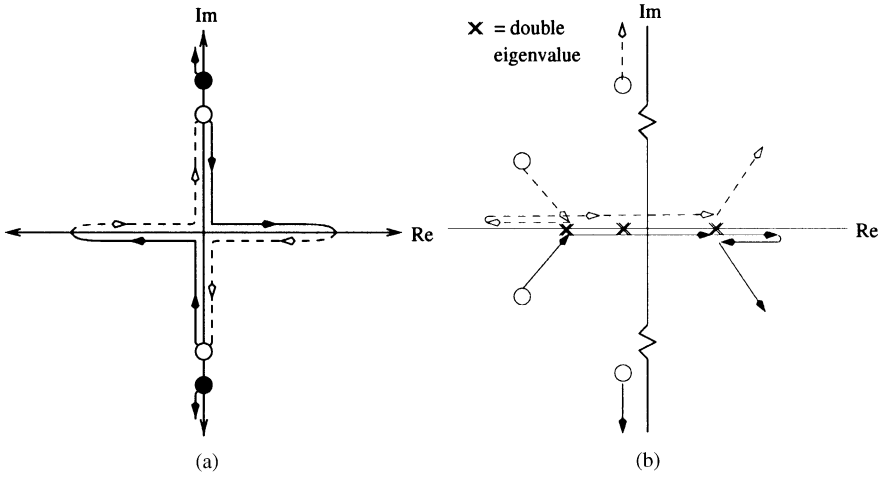

Figure 1. Eigenvalue movement for (a) undamped and (b) damped linear systems.

from damping. Although mechanical systems can have both internal and external damping, we shall focus our attention on internal damping only. We are interested in the effects of periodic perturbations close to the critical point at which the undamped system possesses a double zero eigenvalue. It is well known that, the minimum number of degrees of freedom necessary to incorporate gyroscopic effects is $d = 2$. Furthermore, when damping and non-linearities are added, the two-degree-of-freedom model arises naturally from a center manifold reduction of the continuum model. Therefore, we restrict our attention to the first two modes of vibration, or the first modes in two orthogonal directions in the model of the rotating shaft. It can be shown, as in reference [6], that the essential features of this problem are contained in a two mode truncation of equation (1), i.e., $q \in \mathbb{R}^2$.

The truncated equations of motion can be written in Hamiltonian form,

$$\dot{x} = Lx + JDH_1(x, t) - \zeta[Bx + f(x)],$$

where $x = (q_1, q_2, p_1, p_2)$. After unfolding and calculating the normal form, the equations of motion can be transformed to rectangular coordinates, $x = (x_1, y_1, x_2, y_2)$. These unfoldings and normal form transformations have been performed in some detail in other work [6, 9], so we simply present the equations and a brief description of the bifurcation parameters. The motion of the eigenvalues for the two mode truncated system is shown in Figure 1(a) as the parameter $\Omega = G_{1,2}$ is increased. Note that as Ω is increased, there are two critical points at which the system possesses a non-semisimple double zero eigenvalue. For a S^1 symmetric system, there is only one critical point, a semisimple double zero eigenvalue. As described in reference [6], the normal form used in this paper describes the dynamics near both of these non-semisimple critical cases when the symmetry-breaking is small. The normal form for the unexcited equations of motion near these critical points can be written as

$$\dot{x} = Ax + \zeta Bx + f(x) + \zeta d(x), \tag{2}$$

where $x = (x_1, y_1, x_2, y_2)$. For the excited case, the normal form is given by

$$\dot{x} = \frac{1}{2\Omega}[A_f x + \zeta Bx + f(x) + \zeta d(x)]. \tag{3}$$

Matrix A represents linear conservative terms (Matrix A_f includes linear conservative parametric excitation terms as well), while the matrix B contains linear damping terms. The vector function $f(x)$ contains conservative non-linearities, while the vector $d(x)$ contains non-linear damping terms. In particular, the calculation of the normal form for the forced system requires special techniques, described in Appendix A, to calculate the normal form for a non-autonomous Hamiltonian system. These techniques are described in much more detail in reference [9]. We first present the normal form for the unexcited linear system, followed by the normal form for the excited system, since the latter requires introduction of extra parameters and scalings.

2.1. NORMAL FORM

The goal of this section is to describe the normal form for the general gyroscopic system given in equations (2) or (3). The linear terms in the normal form are given by

$$A = \begin{bmatrix} 0 & \tilde{\delta}+\beta & 0 & 0 \\ \beta-\tilde{\delta} & 0 & 0 & 0 \\ 0 & 0 & 0 & \tilde{\delta}-2\Omega \\ 0 & 0 & -(\tilde{\delta}-2\Omega) & 0 \end{bmatrix}, \quad B = \begin{bmatrix} \frac{\lambda_0}{2\Omega}(\tilde{\delta}-\beta) & 0 & 0 & 0 \\ 0 & \frac{\lambda_0}{2\Omega}(\tilde{\delta}-\beta) & 0 & 0 \\ 0 & 0 & -\zeta\lambda_0 & 0 \\ 0 & 0 & 0 & -\zeta\lambda_0 \end{bmatrix} \tag{4}$$

and, for the excited system (3),

$$A_f = \begin{bmatrix} 0 & \tilde{\delta}-\beta & -\frac{\tilde{h}r_r}{2} & \frac{\tilde{h}r_i}{2} \\ \beta-\tilde{\delta} & 0 & \frac{\tilde{h}r_i}{2} & \frac{\tilde{h}r_r}{2} \\ -\frac{\tilde{h}r_r}{2} & \frac{\tilde{h}r_i}{2} & 0 & \bar{\delta}-2\Omega\tilde{\lambda} \\ \frac{\tilde{h}r_i}{2} & \frac{\tilde{h}r_r}{2} & 2\Omega\tilde{\lambda}-\tilde{\delta} & 0 \end{bmatrix}. \tag{5}$$

The parameter Ω is called the gyroscopic parameter, and is given by $\Omega = G_{1,2} = -G_{2,1}$ from equation (1). For the physical problem of a rotating shaft, Ω is the nominal rotation rate of the shaft, while for the gyroscopic problem of a pipe conveying fluid, Ω is related to the fluid flow rate. The parameter $\tilde{\delta}$ is a bifurcation parameter, measuring the deviation of the gyroscopic parameter Ω from the critical, double zero eigenvalue case. In this problem, $\tilde{\delta}$ was introduced by rewriting Ω and $\Omega = \Omega_c + \tilde{\delta}$, where the trivial solution possesses a non-semisimple double zero eigenvalue at $\Omega = \Omega_c$. The symmetry-breaking parameter β measures how far the system is from being S^1-symmetric (for $\beta = 0$, the system is S^1-symmetric). The parameter ζ measures the damping in the system ($\zeta = 0$ is the undamped case). The coefficient λ_0 is an internal damping coefficient (see reference [6] for details). We assume originally that the parameters $\tilde{\delta}$, ζ, and β are small, $\mathcal{O}(\varepsilon)$, while Ω is $\mathcal{O}(1)$.

For the forced case, $\tilde{h}$ is a forcing parameter, measuring the magnitude of the forcing, while r_i and r_r are forcing coefficients which are related to the physical parameters of the system. We have also introduced the detuning parameter $\tilde{\lambda}$ to measure how far the system is from the critical combination resonance frequency, $\omega_0 = 2\Omega$. The detuning is introduced by rescaling time

$$\tau_1 = 2\Omega(1 - \tilde{\lambda})t.$$

In addition, to eliminate the explicit time-dependence from the forcing terms in the normal form, an additional transformation or rotation has been made which has the side effect of eliminating the term 2Ω in the third and fourth rows of A_f.

The non-linear terms in the normal form are given by

$$f(x) = (x_1^2 + y_1^2)\begin{bmatrix} -A_0 y_1 \\ A_0 x_1 \\ -B_0 y_2 \\ B_0 x_2 \end{bmatrix} + (x_2^2 + y_2^2)\begin{bmatrix} -B_0 y_1 \\ B_0 x_1 \\ -C_0 y_2 \\ C_0 x_2 \end{bmatrix} \tag{6}$$

and

$$d(x) = (x_1^2 + y_1^2)\begin{bmatrix} \alpha_{11} x_1 \\ \alpha_{11} y_1 \\ \alpha_{21} x_2 \\ \alpha_{21} y_2 \end{bmatrix} + (x_2^2 + y_2^2)\begin{bmatrix} \alpha_{12} x_1 \\ \alpha_{12} y_1 \\ \alpha_{22} x_2 \\ \alpha_{22} y_2 \end{bmatrix}, \tag{7}$$

where A_0, B_0, and C_0 are non-linear Hamiltonian coefficients, and α_{ij} are non-linear damping coefficients. For a specific physical problem, these coefficients can be expressed in terms of the physical parameters of the system.

In our analysis, we shall begin with an unforced, undamped linear system, and add the various effects one-by-one. Along the way, we perform scalings to simplify the form of the equations of motion and reduce the number of parameters to be varied. We begin with the unforced linear system in the following section.

2.2. DAMPED, UNFORCED SYSTEM

To simplify this case, we rescale time as $t \to \tau/\beta$ and redefine $\delta = \tilde{\delta}/\beta \sim \mathcal{O}(1)$, $\zeta_1 = \zeta\lambda_0/2\Omega \sim \mathcal{O}(\varepsilon)$, and $\zeta_2 = \zeta\lambda_0/\beta \sim \mathcal{O}(1)$, to obtain

$$A + \zeta B = \begin{bmatrix} \zeta_1(\delta - 1) & \delta - 1 & 0 & 0 \\ 1 - \delta & \zeta_1(\delta + 1) & 0 & 0 \\ 0 & 0 & -\zeta_2 & \delta - \dfrac{2\Omega}{\beta} \\ 0 & 0 & \dfrac{2\Omega}{\beta} - \delta & -\zeta_2 \end{bmatrix}. \tag{8}$$

We note that whereas $\tilde{\delta}$ was $\mathcal{O}(\varepsilon)$, the parameter δ is $\mathcal{O}(1)$. Also, since $\beta \sim \mathcal{O}(\varepsilon)$, the term $2\Omega/\beta \sim \mathcal{O}(1/\varepsilon)$. We also note that since $\zeta \sim \mathcal{O}(\varepsilon)$, the damping in the second mode is

$\mathcal{O}(1)$, while the damping in the first mode $\mathcal{O}(\varepsilon)$. We shall analyze the stability of the unforced conservative system in section 3.1 and the unforced damped system in section 3.2.

2.3. DAMPED FORCED SYSTEM

The equations of motion for the forced system, given by equation (3), are slightly different due to the presence of parametric forcing terms and the need to introduce detuning. We assume originally that the parameters $\tilde{\delta}$, $\tilde{\lambda}$, $\tilde{h}$, β, and ζ are $\mathcal{O}(\varepsilon)$, while Ω, λ_0, r_r, and r_i are $\mathcal{O}(1)$ parameters or coefficients. Also note that the term $(1/2\Omega)\tilde{\lambda}\zeta Bx$ (due to the combined effect of damping and forcing) is $\mathcal{O}(\varepsilon^2)$, and was thus ignored.

Next, we perform scalings and simplifications (similar to those for the unforced case) to put the equations into a more convenient form. We use

$$t \to \frac{2\Omega\tau}{\beta}, \qquad \frac{\tilde{\delta}}{\beta} \to \delta, \qquad \frac{\tilde{h}}{2\beta} - h, \qquad \frac{\tilde{\lambda}}{\beta} \to \lambda$$

and redefine the damping coefficients for the two modes as

$$\zeta_1 = \frac{\zeta\lambda_0}{2\Omega} \sim \mathcal{O}(\varepsilon), \quad \zeta_2 = \frac{\zeta\lambda_0}{\beta} \sim \mathcal{O}(1).$$

Thus, whereas ($\tilde{\delta}$, $\tilde{h}$, $\tilde{\lambda}$) were formerly $\mathcal{O}(\varepsilon)$, the parameters (δ, h, λ) are $\mathcal{O}(1)$, while the symmetry-breaking parameter β remains $\mathcal{O}(\varepsilon)$. For simplicity, we assume that $r_i = 1$, $r_r = 0$, (which is true in the rotating shaft physical example). Then we obtain a rescaled form for the linear matrices A_f and B:

$$A_f = \begin{bmatrix} 0 & \delta + 1 & 0 & h \\ 1 - \delta & 0 & h & 0 \\ 0 & h & 0 & \delta - 2\Omega\lambda \\ h & 0 & 2\Omega\lambda - \delta & 0 \end{bmatrix}, \quad B = \begin{bmatrix} \zeta_1(\delta - 1) & 0 & 0 & 0 \\ 0 & \zeta_1(\delta - 1) & 0 & 0 \\ 0 & 0 & -\zeta_2 & 0 \\ 0 & 0 & 0 & -\zeta_2 \end{bmatrix}. \quad (9)$$

We note that all of the terms are $O(1)$ now, except the damping in the first mode, which is parameterized by $\zeta_1(\delta \pm 1) \sim \mathcal{O}(\varepsilon)$. The analysis of the undamped forced system is undertaken in section 3.3, while the analysis of the forced and damped system, the main topic of this paper, is in section 3.4 and 3.5.

2.4. SCALING OF THE NON-LINEAR TERMS

The terms $f(x)$ and $\zeta d(x)$ in equations (2) and (3) represent the conservative non-linearities and the non-linear damping respectively. Since we will only use the non-linearities to study the forced case, we rescale time as we did for the forced case, and additionally rescale the variables x_i and y_i:

$$t \to \frac{2\Omega\tau}{\beta}, \qquad x_i \to \left(\frac{\beta}{A_0}\right)^{1/2} \tilde{x}_i, \qquad y_i \to \left(\frac{\beta}{A_0}\right)^{1/2} \tilde{y}_i.$$

We shall immediately drop the tildes for convenience. The scalings of the co-ordinates does not affect the linear terms. Thus, the cubic terms are now $\mathcal{O}(\varepsilon)$, and the non-linearities become

$$f(x) = (x_1^2 + y_1^2)\begin{bmatrix} -\gamma y_1 \\ \gamma x_1 \\ -\hat{B}_0 y_2 \\ \hat{B}_0 x_2 \end{bmatrix} + (x_2^2 + y_2^2)\begin{bmatrix} -\hat{B}_0 y_1 \\ \hat{B}_0 x_1 \\ -\hat{C}_0 y_2 \\ \hat{C}_0 x_2 \end{bmatrix} \tag{10}$$

and

$$d(x) = (x_1^2 + y_1^2)\begin{bmatrix} \hat{\alpha}_{11} x_1 \\ \hat{\alpha}_{11} y_1 \\ \hat{\alpha}_{21} x_2 \\ \hat{\alpha}_{21} y_2 \end{bmatrix} + (x_2^2 + y_2^2)\begin{bmatrix} \hat{\alpha}_{12} x_1 \\ \hat{\alpha}_{12} y_1 \\ \hat{\alpha}_{22} x_2 \\ \hat{\alpha}_{22} y_2 \end{bmatrix}, \tag{11}$$

where $\gamma = A_0/|A_0| = \pm 1$, $\hat{B}_0 = B_0/A_0$, $\hat{C}_0 = C_0/A_0$, and $\hat{\alpha}_{ij} = \alpha_{ij}/A_0$. The effect of the non-linearities on the phenomena observed for the linear system will be discussed in section 3.6.

3. STABILITY ANALYSIS

To determine the stability of this system, we will apply the Routh–Hurwitz criterion to the characteristic equations of (8) or (9),

$$s^4 + a_3 s^3 + a_2 s^2 + a_1 s + a_0 = 0,$$

where the coefficients a_i are given in Appendix B. Before studying the stability of the damped and forced system, we study the linear system, the damped linear system, and the forced linear system.

3.1. LINEAR HAMILTONIAN SYSTEM

First we discuss the behavior of the linear system when there is neither forcing nor damping, described by matrix (8) with $\zeta_1 = \zeta_2 = 0$. In this case, the only parameters in the system are the bifurcation parameter δ and the symmetry-breaking parameter β, which we assume is positive, but $\mathcal{O}(\varepsilon)$ small. We shall very δ near zero and observe the motion of the eigenvalues. It is important to note that the eigenvalues of a Hamiltonian system are symmetric about both the real and imaginary axes. The motion of the eigenvalues is shown in Figure 1(a). Because the system is Hamiltonian, we cannot use the Routh–Hurwitz criterion to determine stability. However, it is simple enough to determine stability using the eigenvalues of the system.

The eigenvalues for this system are given by $\lambda_{1,2} = \pm\sqrt{1-\delta^2}$, $\lambda_{3,4} = \pm\,\mathrm{i}(2\Omega/\beta + \delta)$. The second pair of eigenvalues, $\lambda_{3,4}$, remains on the imaginary axis near $\pm\, 2\Omega/\beta$ (far from zero), and move away from each other as δ increases. For $\delta < -1$, the system is stable, as there are two pairs of eigenvalues on the imaginary axis. As δ increases towards -1, $\lambda_{1,2}$

move toward zero. At $\delta = -1$, $\lambda_{1,2}$ reach zero, and they split, causing instability in the system. For $-1 < \delta < 1$, this pair of eigenvalues moves out onto the real axis, changes direction at $\delta = 0$, and returns towards zero. For $\delta = 1$, the system again has a double zero eigenvalue. Finally, for $\delta > 1$, $\lambda_{1,2}$ move away from zero, and their are no further intersections or instabilities. Thus, the important singularities to study occur near $\delta = \pm 1$.

We also note that the parameter variation we study is only one possible parameter variation for a gyroscopic system. In the case of a rotating shaft, the variation of the parameter δ corresponds to a variation in the nominal rotation rate of the shaft. Alternatively, one can vary a parameter corresponding to the axial load. In such a system, the motion of the eigenvalues would be similar, except that, following the double zero eigenvalue situation just described, the two pairs of eigenvalues would approach each other, and the system would become unstable through a Hamiltonian Hopf bifurcation. In a real physical system, the presence of damping always prevents the Hamiltonian Hopf bifurcation from occurring. We do not consider this case here, but rather just study the double zero eigenvalue case.

3.2. DAMPED LINEAR SYSTEM

We now examine the effects of adding damping to the linear Hamiltonian system. In this case, the condition for stability is that all of the eigenvalues be in the left half-plane. The eigenvalues for the damped linear system are

$$\lambda_{1,2} = \delta\zeta_1 \pm \sqrt{1 - \delta^2 + \zeta_1^2}, \quad \lambda_{3,4} = -\zeta_2 \pm i\left(\frac{2\Omega}{\beta} + \delta\right).$$

This eigenvalue motion is shown in Figure 1(b). Since $\zeta_2 > 0$, the eigenvalues $\lambda_{3,4}$ are always in the left half-plane, and far from zero. In fact, these eigenvalues are the eigenvalues $\lambda_{3,4}$ for the undamped case shifted to the left by the amount $|\zeta_2|$. The instability in the system comes from the first pair of eigenvalues, $\lambda_{1,2}$. For $\delta < -\sqrt{1 + \zeta_1^2}$, both of these eigenvalues are in the left half-plane (i.e., negative real parts, and non-zero imaginary parts). At $\delta = -\sqrt{1 + \zeta_1^2}$, the two eigenvalues meet ($\lambda_{1,2} = -\zeta_1\sqrt{1 + \zeta_1^2} < 0$) on the negative real axis, and split, with both eigenvalues remaining on the real axis. One eigenvalue moves further into the left half-plane, and one eigenvalue moves towards the right half-plane, reaching zero and becoming unstable for $\delta \geqslant -1$. The two eigenvalues reverse their direction of motion at $\delta = \pm\zeta_1$, respectively, and meet on the positive real axis ($\lambda_{1,2} = \zeta_1\sqrt{1 + \zeta_1^2} > 0$) at $\delta = \sqrt{1 + \zeta_1^2}$. For $\delta > \sqrt{1 + \zeta_1^2}$, the eigenvalues become imaginary again, with their real parts increasing monotonically. For the damped case, since the eigenvalues meet for the second time in the right half-plane, there is no re-stabilization. Thus, a damped linear gyroscopic system with no forcing will always be unstable for $\delta > -1$. Thus, we will be interested in the singularity near $\delta = -1$, since the singularity near $\delta = +1$ is not physically meaningful.

3.3. FORCED LINEAR HAMILTONIAN SYSTEM

When forcing is added to the system, we introduce a time-dependence into the Hamiltonian terms. We can eliminate the explicit time-dependence by a symplectic time-dependent co-ordinate transformation, i.e., a rotation. This transformation had the

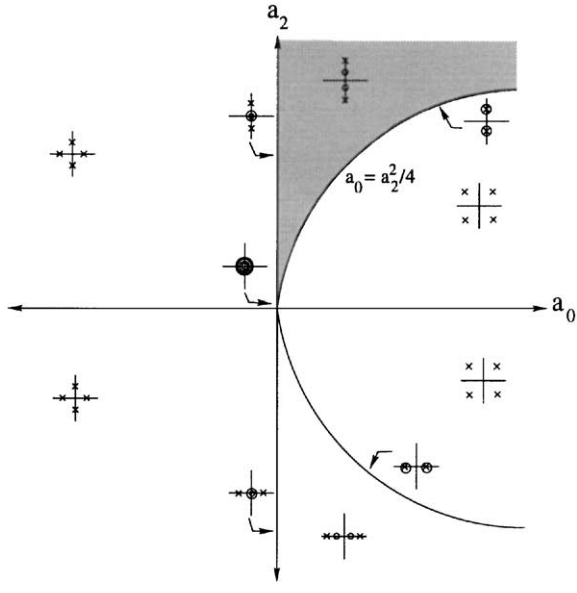

Figure 2. Stability regions for forced Hamiltonian system.

added effect of eliminating the large $2\Omega/\beta$ part of the frequency in $\lambda_{3,4}$. This transformation means that all four eigenvalues will be near zero. The forcing that we add to the system is conservative and can be expressed as part of the Hamiltonian function. The eigenvalues can be determined from the characteristic equation with $\zeta = 0$:

$$s^4 + \tilde{a}_2 s^2 + \tilde{a}_0 = 0.$$

The eigenvalues are then

$$\lambda_{1,2} = \pm \sqrt{\frac{(1-\delta^2) - (\delta - 2\Omega\lambda)^2 + 2h^2 + \sqrt{4h^2(1-4\Omega^2\lambda^2) + (1 - 4\delta\Omega\lambda + 4\Omega^2\lambda^2)^2}}{2}},$$

$$\lambda_{3,4} = \pm i \sqrt{\frac{(\delta^2 - 1) + (\delta - 2\Omega\lambda)^2 - 2h^2 + \sqrt{4h^2(1-4\Omega^2\lambda^2) + (1 - 4\delta\Omega\lambda + 4\Omega^2\lambda^2)^2}}{2}}.$$

The numbering of these eigenvalues correspond to the eigenvalues $\lambda_{1,2,3,4}$ from section 3.1. The paths of the eigenvalues are more difficult to represent, since there are two additional parameters, h and λ. A better method of representation is to plot the stability regions for the system in the h–λ plane for various values of δ. Since we will do the same for the damped and forced linear system in section 3.5, this will provide us with a good basis for understanding the effects of the damping.

From the characteristic equation and symmetry properties, we see that of $\tilde{a}_0 = 0$, then the system possesses two zero eigenvalues (four zero eigenvalues if $\tilde{a}_2 = \tilde{a}_0 = 0$). The system also possesses two coincident pairs of eigenvalues on the imaginary axis if $a_0 = a_2^2/4$. All possible eigenvalue configurations are shown in Figure 2 as a function of a_0 and a_2, where the shaded region is stable.

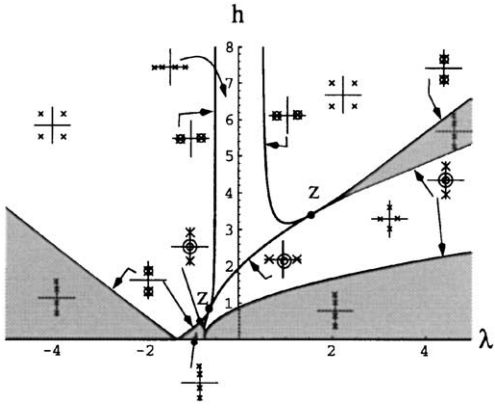

Figure 3. Hamiltonian stability boundary for $\delta = -1{\cdot}5$.

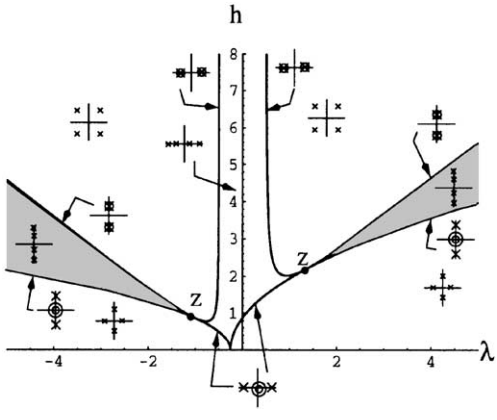

Figure 4. Hamiltonian stability boundary for $\delta = -0{\cdot}5$.

We next plot the curves $a_0 = a_2^2/4$ (Hamiltonian Hopf for $a_2 > 0$, repeated real roots for $a_2 < 0$) and $a_0 = 0$ (double zero, two imaginary roots for $a_2 > 0$, double zero, two real roots for $a_2 < 0$) in the h–λ plane. The curve $a_0 = a_2^2/4$ is given by

$$h_1 = \pm \frac{1 - 4\delta\lambda\Omega + 4\lambda^2\Omega^2}{2\sqrt{4\lambda^2\Omega^2 - 1}}.$$

These curves are undefined for $-1/2\Omega < \lambda < 1/2\Omega$. The curve $a_0 = 0$ is given by

$$h_2 = \pm\sqrt{(\delta - 2\lambda\Omega)(\delta + 1)}, \quad \pm\sqrt{(\delta - 2\lambda\Omega)(\delta - 1)}.$$

Thus, the $a_0 = 0$ curve corresponds to two parabolas in the (h, λ) plane. The two parabolas both open to the right for $\delta < -1$, both open to the left for $\delta > 1$, and one faces each way for $-1 < \delta < 1$. At $\delta = -1$ and $\delta = 1$, one of the parabolas collapses to $h = 0$, and switches from right-facing to left-facing (or *vice versa*). Both parabolas have an offset of $(\delta/2\Omega)$ from the origin of the (h, λ) plane.

We plot the curve of the stability boundaries in the (h, λ) plane for two representative values of δ, $\delta = -1{\cdot}5$ (Figure 3), and $\delta = -0{\cdot}5$ (Figure 4). We only show $h > 0$, since the curves are symmetric about $h = 0$.

In these figures, the stable areas are shaded. The eigenvalue configurations are shown for each of the regions, as well as for the bifurcation surfaces dividing the regions. Note that the points marked "Z" correspond to points at which the system possesses four zero eigenvalues.

For $\delta = -1{\cdot}5$, we can see that the system is only stable below the two curves and in a narrow region for $\lambda > 0$. There are a variety of double zero and Hamiltonian Hopf bifurcations that take place in the system, as well as two points at which the system has four zero eigenvalues. For $\delta = -0{\cdot}5$, the system has only two stable regions, one for $\lambda < 0$ and one for $\lambda > 0$. Again, there are several double zero and Hamiltonian Hopf bifurcations, as well as two points where the system has four zero eigenvalues. Some of the features of these curves will carry over to the case when we have damping and forcing.

As we saw earlier, the addition of damping destroys the re-stabilization of the linear gyroscopic system. Thus, although the undamped system was only unstable for $-1 < \delta < 1$, the damped system is unstable for $\delta > -1$. Now we see that the addition of forcing to the undamped system provides "new" stability regions for $\delta > -1$. The question we will answer next is whether these new stability regions persist when damping is added.

We have to be careful to remember the restrictions we placed on our parameters. For the sake of our perturbative analysis, we required that the parameters $\tilde{\delta}$, $\tilde{h}$, $\tilde{\lambda}$, and $\zeta_{1,2}$ be $\mathcal{O}(\varepsilon)$ initially, while Ω was $\mathcal{O}(1)$. After our scalings, we then had that the parameters, δ, h, and λ were each $\mathcal{O}(1)$. Therefore, we cannot justify these plots for values of δ, h, or λ which are much larger than Ω. To prove that these results hold in such regions would require a more sophisticated analysis.

3.4. ROUTH–HURWITZ CRITERIA FOR DAMPED AND FORCED SYSTEM

The Routh–Hurwitz criteria is a familiar way of determining the number of roots of an equation that have positive real part, i.e., are in the right half-plane. This number is equal to the number of sign changes in the first column of the Routh–Hurwitz table. For the system we are studying, the Routh–Hurwitz table is given in Table 1.

Of course, the first element in the first column, 1, is always positive. The second element, $a_3 = 2(\zeta_2 - \delta\zeta_1)$ is also positive, since $\zeta_2 > 0$, the damping in the second mode, is $\mathcal{O}(1)$, while $\zeta_1 > 0$, the damping in the first mode, is $\mathcal{O}(\varepsilon)$. The third term, b_1, is more complicated. We can show (see Appendix B), that if

$$\zeta_2^2 + 4\Omega^2\lambda^2 - 1 = \mathcal{O}(1), \tag{12}$$

TABLE 1

Routh–Hurwitz table

s^4	1	a_2	a_0
s^3	a_3	a_1	0
s^2	$b_1 = a_2 - \dfrac{a_1}{a_3}$	$b_2 = a_0$	0
s^1	$c_1 = a_1 - \dfrac{a_3 b_2}{b_1} = \dfrac{a_1^2 - a_1 a_2 a_3 + a_0 a_3^2}{a_1 - a_2 a_3}$	0	0
s^0	$d_1 = b_2 = a_0$	0	0

then the sign of b_1 is unimportant in determining the stability or bifurcations of this system. In the case where $\zeta_2^2 + 4\Omega^2\lambda^2 - 1 = \mathcal{O}(\varepsilon)$, the sign of b_1 becomes important. Thus, assuming equation (12) is met, the stability of the system is determined by the last two elements of the first column, c_1 and d_1. Before examining the explicit form of these coefficients, we consider the possibilities for eigenvalues crossing from the left half-plane to the right half-plane (or *vice versa*). There are four non-degenerate cases, as well as degenerate cases:

- $d_1 > 0$, c_1 *passing through zero*: The system goes from having zero sign changes to two sign changes (or *vice versa*). Thus two roots are crossing the imaginary axis, indicating either a Hopf bifurcation or a double zero eigenvalue at $c_1 = 0$. However, a double zero eigenvalue can only occur if $a_1 = a_0 = 0$, contradicting the assumption that $d_1 = a_0 > 0$. Thus, this case refers to a Hopf bifurcation.
- $c_1 > 0$, d_1 *passing through zero*: The system goes from having zero sign changes to one sign change (or *vice versa*). Thus, one root is crossing the imaginary axis, i.e., a simple bifurcation. This is consistent with the fact that the characteristic equation has a zero if $d_1 = a_0 = 0$.
- $d_1 < 0$, c_1 *passing through zero*: There is no change in the number of sign changes in the Routh table, so there is no change in the number of roots in the right half-plane.
- $c_1 < 0$, d_1 *passing through zero*: The system goes from having two sign changes to having only one sign change (or *vice versa*). Thus, one eigenvalue is crossing the imaginary axis, and one eigenvalue remains in the right half-plane. Thus, although there may be a bifurcation involving unstable solutions, there is no change of stability here.
- Degenerate cases: It may happen that both c_1 and d_1 pass through zero at the same time. In this case, the system has a double zero eigenvalue.

Thus, we will sometimes refer to $c_1 = 0$ as the *Hopf condition*, and $d_1 = 0$ as the *simple bifurcation condition*, although a Hopf bifurcation only occurs for ($c_1 = 0$, $d_1 > 0$) and a simple bifurcation only occurs for ($c_1 > 0$, $d_1 = 0$).

In terms of the original system parameters, we can write out the Hopf and simple bifurcation conditions. These conditions are given in Appendix C, and they are quite lengthy. In the following sections, we plot these conditions.

3.5. STABILITY CURVES

Both the Hopf and simple bifurcation curves are given in terms of the three parameters δ, h, and λ, as well as the damping coefficients ζ_1 and ζ_2. To illustrate the stability of the system, we give two different types of stability curves: stability in the h–λ plane, and stability in the δ–λ plane.

3.5.1. *Stability curves in the h–λ plane*

For these curves, we choose $\zeta_1 = 0{\cdot}1$, $\zeta_2 = 2$, and $\Omega = 2$. Similar plots are obtained for different values of the parameters Ω and ζ, as long as equation (12) is satisfied. In this case, we have that $\zeta_2^2 + 4\Omega^2\lambda^2 - 1 \geqslant 3$ for all λ. We plot the conditions $b_1 = 0$, $c_1 = 0$ and $d_1 = 0$ in the h–λ plane for several representative values of δ. Note that since equation (12) is satisfied, the curve $b_1 = 0$ does not affect the stability or bifurcation results, but we show this curve anyway. These curves show the interaction between the two stability conditions, and how the magnitudes of the parameters (δ, h, λ) can affect the type of bifurcations that may occur. We note that the plots are symmetric about $h = 0$, so we only include the

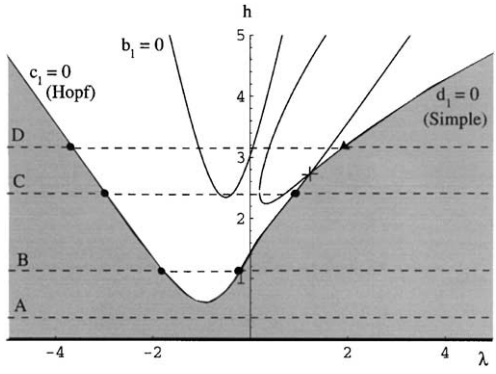

Figure 5. Stability plot for $\delta = -2{\cdot}0$: △, simple bifurcation; ●, Hopf bifurcation; +, double zero eigenvalue.

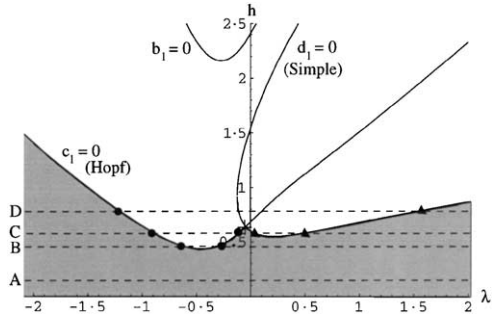

Figure 6. Stability plot for $\delta = -1{\cdot}08$: △, simple bifurcation; ●, Hopf bifurcation; +, double zero eigenvalue.

portion of the plot for $h > 0$. The stability curves for $\delta = -2{\cdot}0$, i.e., for δ far below -1, are given in Figure 5. The shaded regions are stable, and several example paths are shown with constant h and increasing λ. We note that the system is stable below both the Hopf *and* simple bifurcation curves. Along line A, the system is stable for all values of λ. Along line B, the system destabilizes and re-stabilizes through a pair of Hopf bifurcations. Along line C, the system also destabilizes and re-stabilizes through a pair of Hopf bifurcations. However, between the two Hopf bifurcations, one of the unstable eigenvalues passes through zero into the left half-plane and then crosses back into the right half-plane. Along line D, the system again destabilizes through a Hopf bifurcation. The two unstable eigenvalues pass, one at a time, into the left half-plane, and the system thus re-stabilizes through a simple bifurcation. At the point marked " + ", the simple and Hopf curves meet and the system has a double zero eigenvalue. The curve $b_1 = 0$ is above the Hopf curve, and $b_1 > 0$ below that curve. This fact implies that the coefficient b_1 does not affect the bifurcation behavior of the linear system. Finally, we note that the other two eigenvalues always remain in the left half-plane.

At some critical point $\delta = \delta_1^* < -1$, the minimum of the simple bifurcation curve moves outside the Hopf bifurcation curve, changing the bifurcation scenario. The scenario is shown for the typical value $\delta = -1{\cdot}08$ in Figure 6. The analysis is similar to that for the case $\delta = -2{\cdot}0$, except that along line C, the system destabilizes and re-stabilizes through Hopf bifurcations, and then destabilizes and re-stabilizes through simple bifurcations.

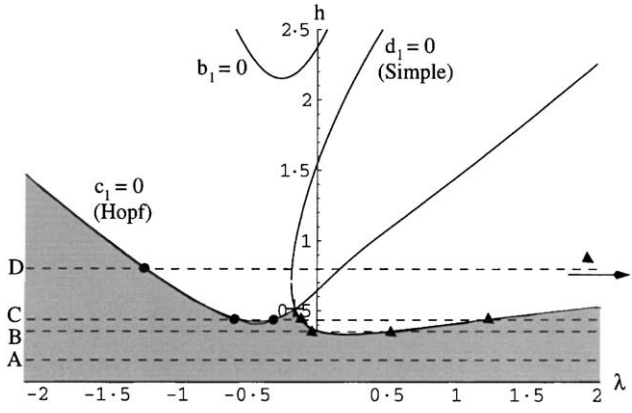

Figure 7. Stability plot for $\delta = -1{\cdot}03$: △, simple bifurcation; ●, Hopf bifurcation; +, double zero eigenvalue.

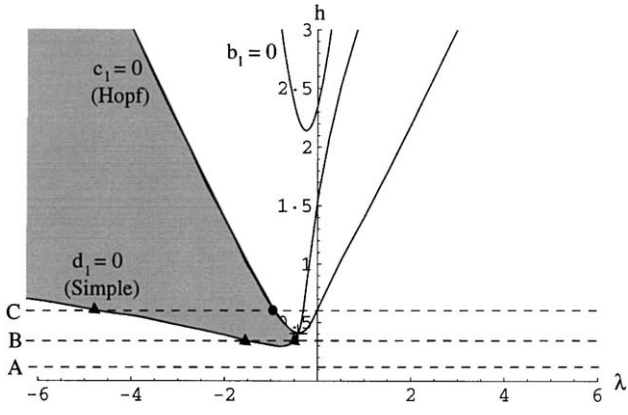

Figure 8. Stability plot for $\delta = -0{\cdot}98$: △, simple bifurcation; ●, Hopf bifurcation; +, double zero eigenvalue.

At another critical point, $\delta = \delta_2^* > \delta_1^*$, the minimum of the simple bifurcation curve moves below the minimum of the Hopf bifurcation curve. This situation is illustrated for $\delta = -1{\cdot}03$ in Figure 7. The bifurcation behavior of this system is similar to the previous two cases, with the following two differences. Along line B, the system destabilizes/re-stabilizes through simple bifurcations. Along line C, the system destabilizes and re-stabilizes through a Hopf bifurcation first, and then a simple bifurcation.

As δ increases towards -1, the right branch of the simple bifurcation curve flattens and swings down, finally reaching $h = 0$ at $\delta = \delta_3^* = -1$. As δ increases past -1, the right branch of the simple bifurcation curve reappears to the left (i.e., for $\lambda < 0$). The Routh coefficient $d_1 = a_0$ is now positive *above* the simple bifurcation curve. Thus the system is now stable only in the region above the simple bifurcation curve and below the Hopf bifurcation curve. (*Note*: For large values of (h, λ), there is another region where stability is possible, as was the case for the undamped, forced system. However, as mentioned earlier, these regions occur for values of (h, λ) which are probably out of the limits of our perturbative analysis. Therefore, we ignore these regions until we can prove their existence more authoritatively.) Such a situation is shown for the typical value of $\delta = -0{\cdot}98$, as shown in Figure 8.

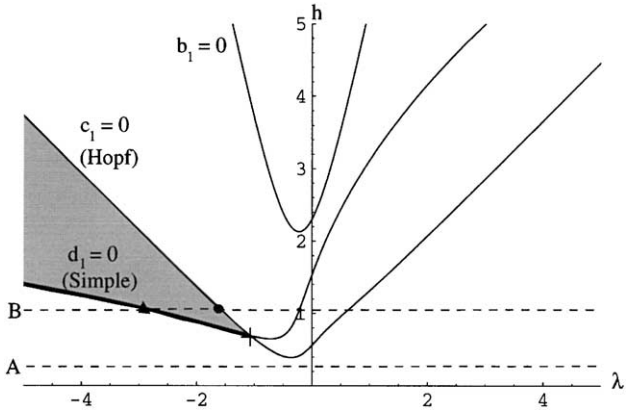

Figure 9. Stability plot for $\delta = -0{\cdot}9$: $\triangle$, simple bifurcation; $\bullet$, Hopf bifurcation; $+$, double zero eigenvalue.

The bifurcation behavior for this case is drastically different from the previous three cases ($\delta = -2{\cdot}0$, $\delta = -1{\cdot}08$, and $\delta = -1{\cdot}03$). The system is now stable only in a wedge above the simple bifurcation curve and below the Hopf curve. Along line A, the system is always unstable. This is the same as for the unforced case (for $\delta > -1$). Along lines B and C, however, there is a region of stability possible. The system is initially unstable for $\lambda \ll 0$, but stabilizes through a simple bifurcation. For higher values of h, the system destabilizes through a Hopf bifurcation. However, since the minimum of the simple bifurcation curve is below the minimum of the Hopf curve, there is a small range of h for which the system destabilizes through a simple bifurcation curve. No re-stabilization is possible, as the system is always unstable for $\lambda > 0$. This is an important result. When the system was damped and unforced, it was always stable for $\delta < -1$ and unstable for $\delta > -1$. Now, where we add forcing, and tune the forcing slightly above the combination resonance frequency, we can obtain stability for $\delta > -1$, albeit only for small regions.

As δ is increased further, the minimum of the simple bifurcation curve moves above the minimum of the Hopf curve, and then moves inside the Hopf curve. The resulting situation is shown in Figure 9 for $\delta = 0{\cdot}9$. In this case, the system becomes stable through a simple bifurcation along line B, and destabilizes through a Hopf bifurcation.

As δ increases, a higher input amplitude is required to obtain this stability region for a given λ. The main difference between Figures 8 and 9 occurs in whether the stability region is destabilized by a Hopf bifurcation or a simple bifurcation. As δ increases further towards zero, the Hopf curve flattens, and finally at $\delta = 0$, the Hopf curve is given by $h = 0$. For $\delta > 0$, the Hopf curve becomes imaginary, which is not physically possible. Since the state of the system must be below the Hopf bifurcation curve to have a chance at being stable, the system cannot be stable for $\delta > 0$.

A possible mechanism for the extended stability region can be explained as follows. In the unforced, damped system, there were two pairs of eigenvalues. One pair of eigenvalues was critical, and became unstable as δ increased through -1. The other pair was far from zero in the left-hand complex plane, and never became unstable. The added parametric excitation at the combination resonance frequency coupled the two modes. The already unstable critical mode was then coupled to the highly damped stable mode. Adding the energy of parametric forcing to an already unstable mode would seem to make the mode even more "unstable". However, through the coupling, energy could be transferred from the unstable mode to the stable mode. Thus, the parametric excitation could allow the already

unstable mode to be stabilized. This stability mechanism may explain why this extended stability region was not observed at the subharmonic parametric resonance frequency.

3.5.2. *Stability curves in the λ–δ plane*

A different view of the extended stability region may be obtained by looking at the stability curves in the λ–δ parameter space, for different values of h. Two such plots, for $h = (0{\cdot}3, 0{\cdot}5)$ are given in Figure 10.

Three curves are shown on these plots. First, there is a vertical curve, $\delta = -1$, which indicates the stability boundary if no parametric excitation is present (i.e., stable for $\delta < -1$, unstable for $\delta > -1$). The second curve, labelled "simple", is the simple bifurcation curve described earlier, i.e., the curve on which the Routh–Hurwitz coefficient $d_1 = 0$. To the left of this curve, $d_1 > 0$, while $d_1 < 0$ to the right of the curve. The other curve, labelled "Hopf", is the Hopf bifurcation curve described earlier. To the left of this curve, the Routh–Hurwitz coefficient $c_1 > 0$, while $c_1 < 0$ to the right. Thus, the system is stable when it is to the left of both the simple and Hopf curves, and unstable when it is to the right of either of these curves.

In these plots, the stable regions are shown as shaded regions. The region we referred to earlier as the "extended stability region" is shown as the darker shaded region. Thus, we see the extended stability region exists for $\lambda < 0$, as before. For $\lambda > 0$, the stability region is reduced. In addition, the extended region of stability (instability) is larger for the higher excitation amplitude h. However, as the amplitude h increases, the stability begins to be affected by the Hopf curve, as part of the Hopf curve moves to the left of the simple curve. This corresponds to the minimum of the simple curve moving above and inside the Hopf curve in the h–λ plots shown earlier.

3.6. EFFECT OF NON-LINEARITIES

The non-linear analysis of this system is greatly complicated by the coupling that exists between the two modes due to the combination resonance forcing. Written in scaled complex co-ordinates, the non-linear equations of motion may be written as

$$\dot{z}_1 = (\delta\zeta - \mathrm{i}\delta)z_1 + (-\zeta + \mathrm{i})\bar{z}_1 + \mathrm{i}h\bar{z}_2 + (\mathrm{i}\gamma + \zeta\alpha_{11})z_1^2\bar{z}_1 + (\mathrm{i}B_0 + \zeta\alpha_{12})z_1z_2\bar{z}_2,$$

$$\dot{z}_2 = [-2\Omega\zeta - \mathrm{i}(\delta - 2\Omega\lambda)]z_2 + \mathrm{i}h\bar{z}_1 + (\mathrm{i}B_0 + \zeta\alpha_{21})z_1z_2\bar{z}_1 + (\mathrm{i}C_0 + \zeta\alpha_{22})z_2^2\bar{z}_2.$$

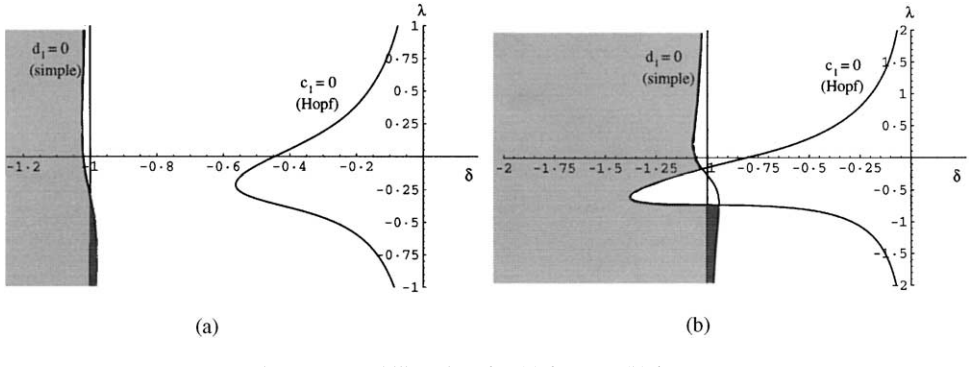

Figure 10. Stability plots for (a) $h = 0{\cdot}3$; (b) $h = 0{\cdot}5$.

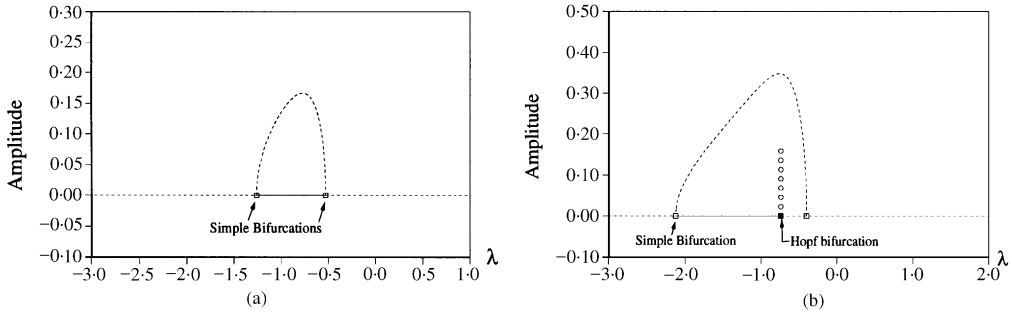

Figure 11. Non-linear bifurcation diagram for (a) $\delta = -0{\cdot}98$, $h = 0{\cdot}4$; (b) $\delta = -0{\cdot}98$, $h = 0{\cdot}5$.

The coupling due to the forcing terms prevents single-mode steady state solutions from existing. For example, to find a first mode solution, we set $z_2 = 0$ and solve for $\dot{z}_1 = 0$ and $\dot{z}_2 = 0$. This yields

$$0 = (\delta\zeta - \mathrm{i}\delta)z_1 + (-\zeta + \mathrm{i})\bar{z}_1 + (\mathrm{i}\gamma + \zeta\alpha_{11})z_1^2\bar{z}_1, \quad 0 = \mathrm{i}h\bar{z}_1.$$

We then conclude that $z_1 = 0$, and we have only the trivial solution ($z_1 = z_2 = 0$). Thus, there can be no single mode solutions, only the trivial solution or multi-mode solutions. These multi-mode solutions are difficult to determine analytically, so we use numerical methods to study the non-linear system.

The extended stability regions we discussed in the previous sections were found for the linear system. Since non-linearities are an important element of any physical system, we would like to observe whether these stability properties persist when non-linear terms are added. We use the numerical bifurcation package AUTO97 [10] to plot bifurcation diagrams for specific cases. AUTO97 allows one to calculate branches of solutions and their stabilities for non-linear systems, given the non-linear coefficients. Although we can not make general statements about the persistence of these results, AUTO97 gives us some verification that the stability results can be extended to the non-linear system.

We look at a pair of bifurcation plots shown in Figure 11 for the full non-linear system. Figure 11(a) corresponds to path B in Figure 8 ($h = 0{\cdot}4$), while Figure 11(b) corresponds to path C in Figure 8 ($h = 0{\cdot}5$). These are plots of the amplitude of the response versus λ. The other parameters are given by ($\Omega = 2$, $\zeta = 0{\cdot}1$, $\zeta_1 = 0{\cdot}1$, $\zeta_2 = 2{\cdot}0$), and the non-linear coefficients (from equations (6) and (7)) are given by ($\gamma = -1$, $\hat{B}_0 = 1{\cdot}3$, $\hat{C}_0 = 2{\cdot}6$, $\hat{\alpha}_{11} = 1{\cdot}0$, $\hat{\alpha}_{12} = 3{\cdot}8$, $\hat{\alpha}_{21} = 3{\cdot}8$, $\hat{\alpha}_{22} = 1{\cdot}9$). In both figures, the trivial solution is initially unstable (dotted line), and stabilizes (solid line) through a simple bifurcation as λ increases. The difference in the two plots is in how the re-stabilized region becomes unstable again: in Figure 11(a), the re-stabilized trivial solution undergoes a simple bifurcation, while in Figure 11(b), the re-stabilized trivial solution undergoes a Hopf bifurcation. Thus, the diagram confirms that this extended stability region may exist for the nonlinear system. The figures also show the unstable solution which bifurcates from the trivial solution, and (in the second figure) the periodic branch which originates from the Hopf bifurcation. We also note that the non-trivial solution branching from the trivial solution is always a multi-mode solution. When there is no forcing at the combination resonance frequency, single-mode solutions are possible.

4. APPLICATION TO ROTATING SHAFT

For weakly damped gyroscopic systems, we have shown that a small periodic forcing, tuned to the right frequency, can extend the domain of stability. This extended stability region is valid when the gyroscopic system has a pair of zero eigenvalues and a pair of imaginary eigenvalues, the input frequency is just above the combination resonance frequency, and the amplitude of the input is sufficiently small.

One physical example of such a gyroscopic system is a rotating shaft, studied before by Shaw and Shaw [11, 12], Nagata and Sri Namachchivaya [6], and McDonald and Sri Namachchivaya [7]. In particular, we have studied a discretized model of a shaft, where we only take the first natural mode in each of the two principal directions. If the shaft is S^1 symmetric, the natural frequencies $\bar{\omega}$ of the shaft are equal for these two principal directions. By choosing a co-ordinate system rotating with the shaft at rate Ω, the frequencies become $\omega_1 = \bar{\omega} - \Omega$ and $\omega_2 = \bar{\omega} + \Omega$. When the rotation rate of the shaft reaches the critical rate $\Omega = \bar{\omega}$, then one of the frequencies, ω_1 becomes zero. In this case, the eigenvalues become 0, 0, and $\pm 2i\Omega$.

The important property, from a stability standpoint, is the natural frequency of the non-rotating shaft, $\bar{\omega}$. Assuming that the shaft is perfectly symmetric, when the rotation rate of the shaft is equal to the shaft's natural frequency, the shaft has a pair of zero eigenvalues. If we break the symmetry assumption, and assume that the shaft is slightly asymmetric, i.e., elliptical, then we introduce a symmetry-breaking parameter β. The effect of the asymmetry on the motion of the eigenvalues is as follows. As the rotation rate of the shaft increases, a pair of eigenvalues becomes zero at $\Omega = \bar{\omega} - \beta$. These eigenvalues split and move onto the real axis (i.e., system becomes unstable), change direction at $\Omega = \bar{\omega}$, and return to zero at $\Omega = \bar{\omega} + \beta$. As the rotation rate is increased further, the eigenvalues remain on the imaginary axis. Thus, the gyroscopic terms allow a re-stabilization of the system.

As has been shown in reference [7], the addition of parametric excitation only influences the dynamics at one of two resonant frequencies. The first resonant frequency is a combination frequency 2Ω which is the sum of the two frequencies 0 and 2Ω. The second frequency is a subharmonic resonance 4Ω which is twice the natural frequency 2Ω. As hypothesized earlier, the extended stability region discussed in this paper relies on the coupling introduced by the combination resonance. Thus, we study only the combination resonance case. To allow the frequency to vary near the critical frequency, we introduce a small detuning parameter λ. The parametric excitation is introduced as a small amplitude periodic perturbation of the rotation rate. The amplitude of this excitation is given by h, and the frequency of the excitation is given by $v = 2\Omega(1 - \varepsilon\lambda)$.

Thus, the main results of this paper translate to the rotating shaft problem as follows. As we showed, the extended stability region exists for δ just larger than -1 (or $-\beta$ in the unscaled system). Also, the stability region only existed for $\lambda < 0$, and for h suitably large. Thus, for the rotating shaft, we would expect to see the extended stability region for a rotation rate slightly greater than $\Omega = \bar{\omega} - \beta$, and an excitation frequency just above the critical combination resonance frequency $v = 2\Omega$. In addition, the amplitude of the excitation would need to be larger than some threshold amplitude.

5. CONCLUSION

In this paper, we have studied a class of weakly damped gyroscopic systems with a weak parametric (periodic) perturbation. These systems were studied near a combination resonance when the undamped system had a pair of zero eigenvalues. For this class of

systems, we have examined the stability of the trivial solution using the Routh–Hurwitz method. We were able to determine the stability and bifurcation behavior of the trivial solution as a function of δ (a bifurcation parameter, e.g., the rotation speed), h (the amplitude of the perturbation), and λ (a detuning parameter from the critical combination resonance).

The unforced, undamped system is stable for $-1 < \delta < 1$. With the addition of forcing and damping, the stability boundaries change. Namely, when the forcing frequency is just above the critical frequency, and the forcing is strong enough, the stability region can be extended so that the system can be stabilized for a range of $\delta > -1$. Conversely, if the forcing frequency is below the critical frequency, the stability region is contracted so that the system is unstable for a range of $\delta < -1$. Using AUTO, it was shown that this behavior may be persistent, i.e. that the expanded stability region persists when non-linearities are added.

A brief discussion was given on how these results might apply to one example of a gyroscopic system, namely a rotating shaft. By tuning the input frequency just above the combination resonance frequency, one might operate at a slightly higher stable rotation speed. Operating at this higher speed might allow some performance gains for the system. Conversely, a stable unforced system might be destabilized by the addition of forcing just below the critical frequency. The results of this research were limited by the approximations taken in our perturbative analysis. Further work that can be done on this problem falls into three categories. First, more precise bounds on where this extended stability region exists should be determined, both for the linear and non-linear systems. Second, we can study the non-linear features of this system which were only briefly touched on in this paper. Finally, experimental verification of this extended stability region would further validate the results of this paper.

ACKNOWLEDGMENTS

The authors would like to acknowledge the support of the Office of Naval Research under grant number N000140110647, and National Science Foundation under grant number CMS 00-84944.

REFERENCES

1. S. T. Ariaratnam and N. Sri Namachchivaya 1986 *Journal of Structural Mechanics* **14**, 127–151. Periodically perturbed linear gyroscopic systems.
2. S. T. Ariaratnam and N. Sri Namachchivaya 1986 *Journal of Structural Mechanics* **14**, 153–175. Periodically perturbed nonlinear gyroscopic systems.
3. S. A. Nayfeh and A. H. Nayfeh 1994 *Journal of Vibration and Acoustics* **116**, 203–207. Energy transfer from high- to low-frequency modes in a flexible structure via modulation.
4. A. H. Nayfeh and D. T. Mook 1999 *Transactions of the American Society of Mechanical Engineers* **186**, 186–195. Energy transfer from high-frequency to low-frequency modes in structures.
5. Z. C. Feng and K. M. Liew 2000 *Nonlinear Dynamics* **21**, 249–263. Global bifurcations in parametrically excited systems with zero-to-one internal resonance.
6. W. Nagata and N. Sri Namachchivaya 1998 *Proceedings of the Royal Society*: *Series A* **454**, 543–585. Bifurcations in gyroscopic systems with an application to rotating shafts.
7. R. McDonald and N. Sri Namachchivaya 1997 *Journal of Chaos, Solitons and Fractals* **8**, 613–636. Global bifurcations in periodically perturbed gyroscopic systems with application to rotating shafts.
8. R. McDonald, J. A. Murdouck and N. Sri Namachchivaya 1999 *Journal of Dynamics and Stability of Systems* **14**, 187–211. Normal forms for nonlinear hamiltonian systems with weak periodic perturbations.

9. R. McDONALD 2000 *Ph.D. Thesis*, University of Illinois at Urbana-Champaign. Bifurcations of Parametrically Excited Gyroscopic Systems Near 0:1 Resonance.
10. E. J. DOEDEL, A. R. CHAMPNEYS, T. F. FAIRGRIEVE, Y. A. KUZNETSOV, B. SANDSTEDE and X. WANG 1997 *AUTO 97 User Manual*. Montreal, Canada: Concordia University. AUTO 97: Continuation and bifurcation software for ordinary differential equations (with homcont).
11. J. SHAW and S. W. SHAW 1989 *Journal of Sound and Vibration* **132(2)**, 227–244. Instabilities and bifurcations in a rotating shaft.
12. J. SHAW and S. W. SHAW 1991 *Journal of Sound and Vibration* **147**, 435–451. Non-linear resonance of an unbalanced rotating shaft with internal damping.
13. V. BARGMANN 1961 *Communications in Pure and Applied Mathematics* **14**, 187–214. On a hilbert space of analytic functions and an associated integral transform.
14. C. ELPHICK, E. TIRAPEGUI, M. E. BRACHET, P. COLLET and G. IOOSS 1987 *Physica D* **29**, 95–127. A simple global characterization for normal forms of singular vector fields.

APPENDIX A: CALCULATION OF NORMAL FORM

In this section, we briefly describe the time-dependent normal form transformation. This transformation is used to simplify the form of the parametric forcing terms in the equations of motion. For more details on this transformation, see reference [8].

Consider a Hamiltonian system given by the equation of motion

$$\dot{x} = J\nabla_x H(\varepsilon, x, t), \tag{A.1}$$

where the Hamiltonian has an expansion

$$H(\varepsilon, x, t) = \sum_{i=0}^{\infty} \frac{\varepsilon^i}{i!} H_i^0(x, t).$$

In particular, H_0^0 is the unperturbed quadratic Hamiltonian, which will be the focus of the normal form. We want to reduce this system, through a symplectic, time-dependent transformation so that the Hamiltonian has a simpler form. It can be shown (see reference [8]) that at each order of the Hamiltonian, an equation of the form

$$\left(\frac{\partial}{\partial t} - D_A^k\right) \mathscr{W}^k = \mathscr{F}^k - \mathscr{G}^k = \Phi^k \tag{A.2}$$

must be solved, where

$$D_A^k = \{H_0^0, \cdot\}, \qquad D_A^k : \mathscr{H}_n^{k,2\pi} \to \mathscr{H}_n^{k,2\pi}$$

and $\{\cdot,\cdot\}$ is the Poisson bracket operator. In equation (A.2), $\mathscr{W}^k$ is the generator of the time-dependent transformation at order k. The actual transformation $x = X(\varepsilon, y, t)$ is the solution of the related Hamiltonian system

$$\frac{\mathrm{d}x}{\mathrm{d}\varepsilon} = J\nabla_x \mathscr{W}(\varepsilon, x, t), \quad x(0) = y$$

with Hamiltonian

$$\mathscr{W}(\varepsilon, x, t) = \sum_{i=0}^{\infty} \frac{\varepsilon^i}{i!} \mathscr{W}^k(x, t).$$

The terms $\mathscr{F}^k$ and $\mathscr{G}^k$ represent kth order terms in the Hamiltonian before the order k normal form transformation, and kth order terms in the normal form. Φ^k is the difference between these two terms, and represents terms which can be eliminated by a time-dependent transformation. The equation is defined on the space $\mathscr{H}_n^{k,2\pi}$, i.e., the space of homogeneous polynomials of degree k in n variables, with 2π periodic coefficients which are C^∞ in t. $\mathscr{W}^k$, $\mathscr{F}^k$, $\mathscr{G}^k$, and Φ^k each belong to $\mathscr{H}_n^{k,2\pi}$. Since the same equation must be solved at each degree k, the superscript k will henceforth only be included when necessary for clarity. We implicitly assume that the perturbations are 2π periodic. Perturbations which are not T-periodic can be handled by scaling so that the perturbations are 2π periodic.

To solve equation (A.2), we first make an isomorphism from $\mathscr{H}_n^{k,2\pi}$ to $C_{2\pi}^\infty(\mathbb{R}, \mathbb{C}^N)$, where N is the number of monomials x^m of degree k in n variables, m being a multi-index. We may enumerate these monomials by $m^{(1)}, m^{(2)}, \ldots, m^{(N)}$. Thus, the space $C_{2\pi}^\infty(\mathbb{R}, \mathbb{C}^N)$ is the space of smooth, 2π periodic mappings of $\mathbb{R}$ into $\mathbb{C}^N$, and represents the space of time-dependent coefficients of elements in $\mathscr{H}_n^{k,2\pi}$. We will use the convention that quantities in $\mathscr{H}_n^{k,2\pi}$ are denoted by (script) capital letters, e.g., $\mathscr{F}$, $\mathscr{G}$, $\mathscr{W}$, and Φ, while the equivalent quantities in $C_{2\pi}^\infty(\mathbb{R}, \mathbb{C}^N)$ will be denoted by small letters, e.g., f, g, w, and ϕ. Thus, for example, an element
$\Phi \in \mathscr{H}_n^{k,2\pi}$, can be written in terms of $\phi \in C_{2\pi}^\infty(\mathbb{R}, \mathbb{C}^N)$ as

$$\Phi = \sum_{j=1}^{N} \phi_j x^{m^j}.$$

Then by regarding $\phi(t) \in \mathbb{C}^N$, the map $\phi : \mathbb{R} \to \mathbb{C}^N$, so that $\phi \in C_{2\pi}^\infty(\mathbb{R}, \mathbb{C}^N)$. Thus, for each element of $\mathscr{H}_n^{k,2\pi}$, there is a corresponding element of $C_{2\pi}^\infty(\mathbb{R}, \mathbb{C}^N)$ representing its time-dependent coefficient, and the correspondence is one-to-one. Thus, considered on the space $C_{2\pi}^\infty(\mathbb{R}, \mathbb{C}^N)$, the partial differential equation (A.2) becomes an ordinary differential equation

$$\frac{\mathrm{d}w}{\mathrm{d}t} - D_A w = f - g = \phi, \tag{A.3}$$

where w, $\phi \in C_{2\pi}^\infty(\mathbb{R}, \mathbb{C}^N)$, and D_A is now in the form of an $N \times N$ matrix, rather than a differential operator. The problem is still infinite dimensional however, since the entries of w and ϕ depend on time.

To solve equation (A.3) and find the normal form g, we note that

$$\phi \in range\left(\frac{\mathrm{d}}{\mathrm{d}t} - D_A\right). \tag{A.4}$$

Then, since $f := g + \phi$, and $f \in C_{2\pi}^\infty(\mathbb{R}, \mathbb{C}^N)$, we must choose g to belong to a complementary subspace to the range in $C_{2\pi}^\infty(\mathbb{R}, \mathbb{C}^N)$. This choice of complementary space is not unique, but the non-uniqueness can be resolved by a particular choice of inner product. To this end, we use an inner product similar to the inner product used earlier for the autonomous case [13, 14], but which accounts for the time-periodic coefficients. Consider two scalar monomials of the form ax^m and bx^l, with $a, b \in C_{2\pi}^\infty(\mathbb{R}, \mathbb{C})$, and m and l are multi-indices. The inner product of these two monomials is defined as

$$\langle ax^m, bx^l \rangle_{\mathscr{H}_n^{k,2\pi}} = \begin{cases} 0, & m \neq l, \\ \dfrac{m!}{2\pi} \int_0^{2\pi} a\bar{b}\, \mathrm{d}t, & m = l, \end{cases} \tag{A.5}$$

where $m!$ is defined as in the autonomous case.

The inner product defined in equation (A.5) takes a simple form when transferred from $\mathscr{H}_n^{k,2\pi}$ to $C_{2\pi}^{\infty}(\mathbb{R}, \mathbb{C}^N)$ by the isomorphism described above. If we let Q be an $N \times N$ diagonal matrix with the diagonal entries given by $q_{jj} = m^{(j)}!$ for $j = 1, \ldots, N$, then the inner product above becomes

$$\langle a, b\rangle_{C_{2\pi}^{\infty}(\mathbb{R}, \mathbb{C}^N)} = \frac{1}{2\pi} \int_0^{2\pi} b^* Q a \, \mathrm{d}t, \tag{A.6}$$

where now $a, b \in C_{2\pi}^{\infty}(\mathbb{R}, \mathbb{C}^N)$. Using the inner product (A.5) or (A.6), and well-known results of linear analysis allow us to calculate a simpler form for the adjoint operator,

$$\left(\frac{\mathrm{d}}{\mathrm{d}t} - D_A\right)^* = -\left(\frac{\mathrm{d}}{\mathrm{d}t} + D_{A^*}\right) = -\left(\frac{\mathrm{d}}{\mathrm{d}t} + D_{S^*} + D_{N^*}\right).$$

We can also show the following important properties [8]:

(1) range $(\frac{\mathrm{d}}{\mathrm{d}t} - D_A) = ker(-\frac{\mathrm{d}}{\mathrm{d}t} - D_{A^*})^{\perp} = ker\,(\frac{\mathrm{d}}{\mathrm{d}t} + D_{A^*})^{\perp}$,
(2) $ker\,(\frac{\mathrm{d}}{\mathrm{d}t} + D_{A^*}) = ker\,(\frac{\mathrm{d}}{\mathrm{d}t} + D_{S^*}) \cap ker\,(D_{N^*})$,

which are essential to the treatment of the time-periodic normal form. This allows us to choose an orthogonal complementary space to *range* $(\mathrm{d}/\mathrm{d}t - D_A)$ to be the kernel of the adjoint operator, i.e., the normal form

$$g \in ker\left(\frac{\mathrm{d}}{\mathrm{d}t} - D_A\right)^* = ker\left(\frac{\mathrm{d}}{\mathrm{d}t} + D_{A^*}\right). \tag{A.7}$$

It is worth noting that we can not simply apply the Fredholm alternative to prove this, since we cannot easily prove that the linear operator is Fredholm.

Hence, as shown in reference [8], these properties give a straightforward method for determining the normal form $g \in ker\ (\mathrm{d}/\mathrm{d}t - D_A)^*$. First, determine a basis $\{w_i\}$ for the kernel of the semisimple operator $\mathscr{S} = (\mathrm{d}/\mathrm{d}t + D_{S^*})$. Then find $(D_{N^*})|_{\ker(\mathscr{S})}$, i.e., the action of the nilpotent operator $\mathscr{N} = D_{N^*}$ on this basis $\{w_i\}$. Then, find a basis $\{v_i\}$ for the kernel of $(D_{N^*})|_{\ker(\mathscr{S})}$. This basis $\{v_i\}$ provides a basis for the normal form, since it belongs both to $\ker \mathscr{S}$ and $\mathrm{Ker}\,\mathscr{N}$.

The coefficients of these normal form terms can then be determined by projecting the original terms, f, onto the space spanned by the normal form. Thus, if $\{v_i\}$ is a basis for the normal form, and α_i are the corresponding unknown coefficients, then the α_i can be found from the equation

$$\langle f - \alpha_i v_i, v_j\rangle_{C_{2\pi}^{\infty}(\mathbb{R}, \mathbb{C}^N)} = 0 \tag{A.8}$$

or, if the basis for the kernel is an orthogonal one, then

$$\alpha_i = \frac{\langle f, v_i\rangle_{C_{2\pi}^{\infty}(\mathbb{R}, \mathbb{C}^N)}}{\langle v_i, v_i\rangle_{C_{2\pi}^{\infty}(\mathbb{R}, \mathbb{C}^N)}}. \tag{A.9}$$

Choosing the coefficients in this way ensures that the homological equation has a solution.

Finally, the solution for the generating function w is given by the solution of the ordinary differential equation (A.3), i.e.,

$$w(t) = e^{D_A t} w_0 + \int_0^t \mathrm{e}^{D_A(t-\tau)} \phi(\tau)\, \mathrm{d}\tau, \tag{A.10}$$

where $\mathrm{e}^{D_A t}$ is a fundamental matrix solution of the homogeneous equation. The initial condition w_0 can be specified by requiring the solution of this equation to be a 2π periodic function of time, i.e.,

$$w_0 = \mathrm{e}^{2\pi D_A}\left[w_0 + \int_0^{2\pi} \mathrm{e}^{-D_A \tau} \phi(\tau)\, \mathrm{d}\tau \right],$$

$$(I - \mathrm{e}^{2\pi D_A}) w_0 = \int_0^{2\pi} \mathrm{e}^{D_A(2\pi - \tau)} \phi(\tau)\, \mathrm{d}\tau. \tag{A.11}$$

Finally, we make the isomorphism from the space of time-dependent coefficients, $C^\infty_{2\pi}(\mathbb{R}, \mathbb{C}^N)$, back to the space of homogeneous polynomials, $\mathscr{H}^{k,2\pi}_n$ to determine the normal form and transformations in terms of monomials. Thus, we have given a complete procedure for obtaining the solutions for the normal form, the normal form coefficients, and the generators of the transformations. These computations were possible due to the fact that for periodic systems, one can reduce the infinite dimensional problem to a finite dimensional one. In the next section, we provide an example to illustrate these ideas, but first, we mention an alternate characterization of this normal form.

Theorem A.1. (Alternate characterization of normal form). *The normal form* $K^i_0\,(i = 1, 2, \dots)$ *has the following property*:

$$K^i_0(\mathrm{e}^{-A^* t} x, t) = K^i_0(x, 0), \quad i = 1, 2, \dots,$$

where A^* *is the adjoint, or conjugate transpose of* A.

Another way of looking at this alternate characterization is to observe that the terms in the normal form are invariant under the flow of $\mathrm{e}^{-A^* t}$. Additionally, when the system is semisimple, then the unperturbed term K^0_0 will also satisfy this property, i.e., $K^0_0(\mathrm{e}^{-A^* t} z, t) = K^0_0(z, 0)$. In this case, we can use the transformation $x = \mathrm{e}^{-A^* t} z$ to eliminate the time-dependence in the higher order terms, leaving the unperturbed term K^0_0 unchanged. This simplification does not work for the non-semisimple case, since the transformation would introduce time-dependence into the unperturbed term K^0_0. However, we show that

$$K^i_0(\mathrm{e}^{-S^* t} z, t) = K^i_0(z, 0), \quad i = 0, 1, 2, \dots,$$

where S is the semisimple part of matrix A. Since this property holds even for K^0_0, we can use the transformation

$$x = \mathrm{e}^{-S^* t} z$$

to eliminate the time-dependence from the higher order terms while leaving K_0^0 unchanged. This transformation will be demonstrated in the example problem.

APPENDIX B: NON-LINEAR COEFFICIENTS

Here we display the relationships between the non-linear coefficients obtained in the normal form and the original non-linear coefficients of the system.

The conservative non-linearity in the original equations was given by

$$U(q, p) = U_0(q, p) + U_\delta(q, p) + U_\beta(q, p),$$

where

$$\begin{aligned} U_0(q, p) = {} & \frac{a_1}{4}(q_1^2 + q_2^2)^2 + \frac{a_2}{4}(p_1^2 + p_2^2)^2 + \frac{a_3}{4}(q_1^2 + q_2^2)(q_1 p_1 + q_2 p_2) \\ & + \frac{a_4}{4}(p_1^2 + p_2^2)^2(q_1 p_1 + q_2 p_2) + \frac{a_5}{4}(q_1 p_1 + q_2 p_2)^2 + \frac{a_6}{4}(q_1 p_2 - q_2 p_1)^2 \\ & - \frac{a_7}{4}(q_1^2 + q_2^2)(q_1 p_2 - q_2 p_1) - \frac{a_8}{4}(p_1^2 + p_2^2)(q_1 p_2 - q_2 p_1) \\ & - \frac{a_9}{4}(q_1 p_2 - q_2 p_1)(q_1 p_1 + q_2 p_2), \end{aligned}$$

$$\begin{aligned} U_\delta(q, p) = \delta \Big\{ & \frac{b_1}{4}(q_1^2 + q_2^2)^2 + \frac{b_2}{4}(p_1^2 + p_2^2)^2 + \frac{b_3}{4}(q_1^2 + q_2^2)(q_1 p_1 + q_2 p_2) \\ & + \frac{b_4}{4}(p_1^2 + p_2^2)(q_1 p_1 + q_2 p_2) + \frac{b_5}{4}(q_1 p_1 + q_2 p_2)^2 + \frac{b_6}{4}(q_1 p_2 - q_2 p_1)^2 \\ & - \frac{b_7}{4}(q_1^2 + q_2^2)(q_1 p_2 - q_2 p_1) - \frac{b_8}{4}(p_1^2 + p_2^2)(q_1 p_2 - q_2 p_1) \\ & - \frac{b_9}{4}(q_1 p_2 - q_2 p_1)(q_1 p_1 + q_2 p_2) \Big\} \end{aligned}$$

and

$$U_\beta(q, p) = \frac{\beta}{4}[c_1 q_1^4 + c_2 q_1^3 q_2 + c_3 q_1^2 q_2^2 + c_4 q_1 q_2^3 + c_5 q_2^4].$$

The term $U_0(q, p)$ is the most general S^1 symmetric non-linearity of fourth order, and $U_\delta(q, p)$ is a perturbation due to the bifurcation parameter δ. The term $U_\beta(q, p)$ is a general

fourth order perturbation which breaks the symmetry. The original damping terms are given by

$$d(x) = [0 \;\; 0 \;\; d_1(q, p) \;\; d_2(q, p)]^{\mathrm{T}},$$

where

$$d_1(q, p) = (\xi_1 q_1 + \xi_4 q_2)(q_1 p_1 + q_2 p_2) - (\xi_2 q_2 + \xi_3 q_1)(\Omega q_2^2 + q_2 p_1 + \Omega q_1^2 - q_1 p_2),$$

$$d_2(q, p) = (\xi_1 q_2 + \xi_4 q_1)(q_1 p_1 + q_2 p_2) + (\xi_2 q_1 - \xi_3 q_2)(\Omega q_2^2 + q_2 p_1 + \Omega q_1^2 - q_1 p_2).$$

The original non-autonomous terms are given by

$$H(q, p, t) = H_0(q, p, t) + H_\delta(q, p, t) + H_\beta(q, p, t),$$

where

$$H_0(q, p, t) = \mu \cos(\nu t)[e_1(q_1^2 + q_2^2) + e_2(p_1^2 + p_2^2) + e_3(q_1 p_1 + q_2 p_2) + e_4(q_2 q_1 - q_1 p_2)],$$

$$H_\delta(q, p, t) = \delta\mu \cos(\nu t)[\varepsilon_1(q_1^2 + q_2^2) + \varepsilon_2(p_1^2 + p_2^2) + \varepsilon_3(q_1 p_1 + q_2 p_2) + \varepsilon_4(q_2 p_1 - q_1 p_2)],$$

$$\begin{aligned} H_\beta(q, p, t) = \beta\mu \cos(\nu t)[&f_1 q_1^2 + f_2 q_1 q_2 + f_3 q_1 p_1 + f_4 q_1 p_2 + f_5 q_2^2 + f_6 q_2 p_1 \\ &+ f_7 q_2 p_2 + f_8 p_1^2 + f_9 p_1 p_2 + f_{10} p_2^2]. \end{aligned}$$

The term $H_0(q, p, t)$ is a general S^1 symmetric perturbation, $H_\delta(q, p, t)$ is a perturbation of the forcing due to the bifurcation parameter δ and $H_\beta(q, p, t)$ is a perturbation of the forcing which breaks the symmetry. The non-linear and forcing coefficients that appear in the normal form that we study are γ, B_0, C_0, α_{11}, α_{12}, α_{21}, α_{22}, r_i, r_r. The non-linear Hamiltonian coefficients are

$$A_0 = \frac{a_1}{\Omega^2} + a_2\Omega^2 + a_6 - \frac{a_7}{\Omega} - a_8\Omega \quad B_0 = \frac{2a_1}{\Omega^2} + 2a_2\Omega^2 + a_5 - a_6,$$

$$C_0 = \frac{a_1}{\Omega^2} + a_2\Omega^2 + a_6 + \frac{a_7}{\Omega} + a_8\Omega.$$

The damping coefficients are

$$\alpha_{11} = \mathrm{Re}(A) - \frac{\lambda_0 E_0}{4\Omega}, \quad \alpha_{12} = \mathrm{Re}(B_1) - \frac{\lambda_0 F_0}{2\Omega},$$

$$\alpha_{21} = \mathrm{Re}(B_2) + \frac{\lambda_0 E_0}{2\Omega}, \quad \alpha_{22} = \mathrm{Re}(C) + \frac{\lambda_0 F_0}{2\Omega},$$

where the new coefficients A, B_1, B_2, and C may be given in terms of the original damping coefficients ξ_i, $i = 1, 2, 3, 4$ and

$$E_0 = \frac{2a_1}{\Omega^2} - 2a_2\Omega^2 - \frac{a^7}{\Omega} + a_8\Omega, \quad F_0 = \frac{2a_1}{\Omega^2} - 2a_2\Omega^2 + \frac{a^7}{\Omega} + a_8\Omega.$$

Finally, the non-autonomous coefficients are

$$r = r_{1100} = r_{1100_i} + r_{1100_r} = r_i + r_r, \quad r_i = \frac{e_1}{\Omega} - e_2\Omega, \quad r_r = -e_3.$$

APPENDIX C: COEFFICIENTS OF CHARACTERISTIC EQUATION AND ROUTH TABLE

First, we give the coefficients of the characteristic equation for the unforced case, where the linear matrix is given by equation (8). The coefficients are

$$a_4 = 1, \quad a_3 = 2\zeta_2 - 2\delta\zeta_1,$$

$$a_2 = (\delta^2 - 1) + (\delta - 2\Omega/\beta)^2 + \zeta_1^2(\delta^2 - 1) - 4\delta\zeta_1\zeta_2 + \zeta_2^2,$$

$$a_1 = -2\delta\zeta_1(\delta - 2\Omega/\beta)^2 + 2\zeta_2(\delta^2 - 1) + 2\zeta_1\zeta_2((\delta^2 - 1)\zeta_1 - \delta\zeta_2),$$

$$a_0 = (\delta^2 - 1)(1 + \zeta_1^2)((\delta - 2\Omega/\beta)^2 + \zeta_2^2).$$

The characteristic equation for the undamped case is obtained by simply setting $\zeta_1 = \zeta_2 = 0$ in the above coefficients. In particular, for the undamped case, $a_3 = a_1 = 0$.

The coefficients of the characteristic equation for the forced case, where the linear matrix is given by equation (9), are

$$a_4 = 1, \quad a_3 = 2\zeta_2 - 2\delta\zeta_1,$$

$$a_2 = (\delta^2 - 1) - 2h^2 + (\delta - 2\Omega\lambda)^2 + \zeta_1^2(\delta^2 - 1) - 4\delta\zeta_1\zeta_2 + \zeta_2^2,$$

$$a_1 = 2\delta\zeta_1(h^2 - (\delta - 2\Omega\lambda)^2) + 2\zeta_2(\delta^2 - 1 - h^2) + 2\zeta_1\zeta_2((\delta^2 - 1)\zeta_1 - \delta\zeta_2),$$

$$a_0 = h^4 - 2\delta h^2(\delta - 2\Omega\lambda - \zeta_1\zeta_2) + (\delta^2 - 1)(1 + \zeta_1^2)((\delta - 2\Omega\lambda)^2 + \zeta_2^2).$$

Next, we examine the entries in the Routh–Hurwitz table given as Table 1 at the beginning of section 3.4.

First, we have

$$a_3 = 2(\zeta_2 - \delta\zeta_1).$$

We note that $\zeta_2 > 0$ is $\mathcal{O}(1)$, while $\zeta_1 > 0$ is $\mathcal{O}(\varepsilon)$. Therefore, a_3 will always be positive. Next, we examine the terms b_1 and c_1. Using the scaling $\zeta_1 \to \varepsilon\zeta_1$, we can determine

approximations for the curves $b_1 = 0$ and $c_1 = 0$:

$$h_{b_1}^2 = (\delta - 2\Omega\lambda)^2 + \zeta_2^2 + \mathcal{O}(\varepsilon),$$

$$h_{c_1}^2 = \varepsilon \frac{-\delta\zeta_1(\zeta_2^4 + (1 - 4\delta\lambda\Omega + 4\Omega^2\lambda^2)^2 + 2\zeta_2^2((\delta^2 - 1) + (\delta - 2\Omega\lambda)^2))}{\zeta_2(\zeta_2^2 + 4\Omega^2\lambda^2 - 1)} + \mathcal{O}(\varepsilon^2).$$

Normally, these approximations would allow us to conclude that

$$h_{b_1}^2 - h_{c_1}^2 = (\delta - 2\Omega\lambda)^2 + \zeta_2^2 + \mathcal{O}(\varepsilon).$$

The only problem is when the denominator of the $\mathcal{O}(\varepsilon)$ term of $h_{c_1}^2$ approaches zero. Thus, we require that

$$\zeta_2^2 + 4\Omega^2\lambda^2 > 1.$$

If we have that $\zeta_2^2 + 4\Omega^2\lambda^2$ is just above 1, then the Hopf curve will have a peak near $\lambda = 0$. If, in fact, we have that $\zeta_2^2 + 4\Omega^2\lambda^2 < 1$ for a range of λ, then the Hopf curve is undefined for the range $-\lambda_1 < \lambda < \lambda_1$, where

$$\lambda_1 = \sqrt{\frac{1 - \zeta_2^2}{4\Omega^2}}.$$

We shall not consider this case in detail, but the method of analysis using the Routh criterion is similar. Thus, we shall require that

$$\zeta_2^2 + 4\Omega^2\lambda^2 - 1 \geqslant \mathcal{O}(1).$$

Under this condition, the curve $b_1 = 0$ is above the curve $c_1 = 0$ in the $h^2 - \lambda$ plane. Note that the minimum distance between the two curves occurs at $\lambda = \delta/2\Omega$ and is given by ζ_2^2. Furthermore, $b_1 < 0$ ($b_1 > 0$) above (below) the curve $b_1 = 0$, and $c_1 < 0$ ($c_1 > 0$) above (below) the curve $c_1 = 0$. Hence, if $b_1 < 0$ at a point in the $h^2 - \lambda$, then that point is above the $c_1 = 0$ curve, and thus $c_1 < 0$ as well. Returning to the Routh–Hurwitz table, it is obvious that if $a_3 > 0$ and $c_1 < 0$, then the sign of b_1 has no effect on the number of sign changes in the first column of the Routh table, and hence no effect on the number of roots in the right half-plane.

APPENDIX D: HOPF AND SIMPLE BIFURCATION CONDITIONS

The simple bifurcation condition is given by

$$d_1 = h^4 - 2h^2\delta(\delta - 2(\zeta^2 + \lambda)\Omega) - (1 - \delta^2)(1 + \zeta^2)(\delta^2 - 4\delta\lambda\Omega + 4(\zeta^2 + \lambda^2)\Omega^2).$$

Solving this for $h^2 = h^2(\lambda, \delta, \Omega, \zeta)$, we obtain

$$h^2 = \frac{1}{2}\{2\delta[\delta - 2(\zeta^2 + \lambda)\Omega]$$

$$\pm \sqrt{4\delta^2[\delta - 2(\zeta^2 + \lambda)\Omega]^2 - 4(\delta^2 - 1)(1 + \zeta^2)(\delta^2 - 4\delta\lambda\Omega + 4(\zeta^2 + \lambda^2)\Omega^2)}\}.$$

The Hopf bifurcation condition is given by

$$c_1 = \frac{1}{\delta(1 - \delta^2)(1 + \zeta^2) + (h^2 + 8\delta\zeta^2\Omega)(\delta - 2\Omega) + (2\delta\Omega - 4\lambda\Omega^2)(\delta - 2\lambda\Omega) + 8\zeta^2\Omega^3}$$

$$\times\{ -2\zeta[h^2(\delta - 2\Omega)^2(\delta^2\zeta^2 - (1 + \zeta^2) - 4\delta\zeta^2\Omega + 4(\zeta^2 + \lambda^2)\Omega^2)$$

$$+ 2\delta\Omega((1 + \zeta^2)^2 + \delta^4\zeta^2(4 + \zeta^2) - 8\delta^3\zeta^2(2 + \zeta^2 + \lambda)\Omega$$

$$+ 8\delta^2(2\zeta^2 + 3\zeta^4 + 4\zeta^2\lambda + 2\lambda^2 + \zeta^2\lambda^2)\Omega^2 - 32\delta(\zeta^4 + \zeta^2\lambda + \zeta^2\lambda^2 + \lambda^3)\Omega^3$$

$$+ 16(\zeta^2 + \lambda^2)^2\Omega^4 - 2(1 + \zeta^2)(\delta^2\zeta^2 + 4\delta(\lambda - \zeta^2)\Omega + 4(\zeta^2 - \lambda^2)\Omega^2))]\}$$

and the solution for $h^2 = h^2(\lambda, \delta, \Omega, \zeta)$, though long, can be easily found.